 doi:10.20944/preprints202208.0477.v1

Article

LiDAR and UAV SfM-MVS of Merapi Volcanic Dome & Crater Rim Change from 2012 to 2014

Christopher Gomez [1,2,*], Franck Lavigne [3], Muhammad Anggri Setiawan [2,4], Noviyanti Listyaningrum [2,4], Sandy Budi Wibowo [5], Danang Sri Hadmoko [2,4], Wiwit Suryanto [6], Herlan Darmawan [6], Balazs Bradak [1], Rikuto Daikai [1], Sunardi Sunardi [7,8], Yudo Prasetyo [9], Annisa Joviani Astari [10], Lukman Lukman [11], Idea Wening Nurani [3,12], Moh. Dede [8], Indranova Suhendro [2,4]

1 Kobe University, Faculty of Oceanology, Laboratory of Sediment Hazards and Disaster Risks; christopher-gomez@bear.kobe-u.ac.jp (C.G.), bradak.b@port.kobe-u.ac.jp (B.B.)
2 Center for Disaster Study, Universitas Gadjah Mada, Indonesia; anggri.setiawan@gmail.com
3 Université Paris 1 Panthéon-Sorbonne, Laboratory of Physical Geography UMR 8591, France; franck.lavigne@univ-paris1.fr (F.L.), Idea-Wening.Nurani@etu.univ-paris1.fr (I.W.N.)
4 Department of Environmental Geography, Faculty of Geography, Universitas Gadjah Mada, Indonesia; hadmoko@ugm.ac.id (D.S.H), noviyanti.listyaningrum@mail.ugm.ac.id (N.L.), indranova.suhendro@mail.ugm.ac.id (I.S.)
5 Department of Geographic Information Science, Faculty of Geography, Universitas Gadjah Mada, Indonesia; sandy_budi_wibowo@ugm.ac.id
6 Faculty of Mathematics and Natural Sciences, Universitas Gadjah Mada, Indonesia; ws@ugm.ac.id (W.S.), herlan_darmawan@mail.ugm.ac.id (H.D.)
7 Faculty of Mathematics and Natural Sciences, Universitas Padjadjaran, Indonesia; sunardi@unpad.ac.id
8 Doctoral Program on Environmental Science, Postgraduate School (SPs), Universitas Padjadjaran, Indonesia; m.dede.geo@gmail.com
9 Department of Geodetic Engineering, Faculty of Engineering, Universitas Diponegoro, Indonesia; yudo.prasetyo@ft.undip.ac.id
10 Faculty of Social Science Education, Geographic Information Science Study Program, Universitas Pendidikan Indonesia, Indonesia; annisa.astari@upi.edu
11 National Research and Innovation Agency (BRIN), Indonesia; lukm001@brin.go.id
12 Department of Development Geography, Faculty of Geography, Universitas Gadjah Mada, Indonesia; idea.nurani@ugm.ac.id

* Correspondence: christophergomez@bear.kobe-u.ac.jp;

Abstract: Spatial approach based on the deformation measurement of volcanic dome and crater rim is key to evaluate the activity of a volcano, such as Merapi volcano where associated disaster risk is regularly taking lives. Within this framework, this study aime to detect localized deformation and change in the summit area that has occurred concomitantly with the dome growth and explosion reported. The methodology was focused on two sets of data, one LiDAR-based dataset of 2012 and one UAV-dataset of 2014. The results show that during the period 2012-2014, the crater walls are 100 m to 120 m high above the crater floor at its maximum (North to East-South-East sector), while the West and North sector presents a topographic range of 40 to 80 m. During the period 2012 – 2014, the evolution of the crater rim around the dome is generally stable (no large collapse). The opening of a new vent on the surface of the dome has displaced an equivalent volume of 2.04 E+04 m^3 corresponding to a maximum -9 m (+/- 0.9 m) vertically. This concludes that during the period 2012 – 2014 when the dome of Merapi experienced phreatic or phreatomagmatic explosions, the topography around the dome rose. This rise does not seem to be related to large wall collapses, and it is likely that modification in the subsurface have triggered those changes.

Keywords: Merapi Volcano; Indonesia; Natural Hazards; Disaster Risk and Point-cloud technology

1. Introduction

 doi:10.20944/preprints202208.0477.v1

On stratovolcanoes, domes are a major source of hazards as they often collapse under both the action of internal gas pressure [1] and gravity [2], to create hazardous pyroclastic-density currents [3]. Without gravitational collapses, internal gas pressure can generate explosive eruptions eventually propelling ash and other volcanic material up in the upper atmosphere, in addition to which, chemically stable domes can still explode by phreatic and phreatomagmatic processes [4]. Even during the more quiescent phase, volcanic domes are still evolving, eventually sliding away from the top of the volcano [5], and breaking apart into "smaller pieces", generating long-runout rockfalls [6]. Environmental factors of the dome also contribute to the dome instability: for instance, precipitation contributing to hydrothermal alteration; the general movement of the volcanic structure (uplift and subsidence) as well as the local and regional seismic activity (from Vazquez *et al.* after the work of McGuire [7]). But, as it was recently pointed out, despite a variety of explaining factors, the contribution of one over another still remains scientifically unclear [8]. For the purpose of disaster risk management, and to avoid catastrophe, dome monitoring is thus essential, even during periods that are more quiescent.

In Central Java, Indonesia, a series of dome-collapse pyroclastic density-currents have been sweeping the flanks of Merapi Volcano during the Holocene period, although larger eruptions and sector collapses are also found in the earlier Quaternary period, known since ~360,000 BP [9,10]. The pyroclastic density-currents of the last major eruption in 2010 (VEI4: [11]) have covered an area of 22.3 km^2 [12,13], in turn turning into lahars that have flooded the valleys towards Yogyakarta City [14,15], and in its aftermath the growth of the dome also generated rockfall hazards [6].

Consequently, the evolution of the dome has attracted the attention of scientists in different fields of research, e.g. rock geochemistry [16], gaz analysis [17], numerical modeling [18], petrology [19], surface deformation [20,21], and seismology [22]. During the historical period, the dome of Merapi Volcano has been lodged into a horseshoe crater-rim, opened towards the South, directing most of the gravity collapse pyroclastic-flows and rockfalls [6], locally called '*guguran*' in this same direction (Figure 1).

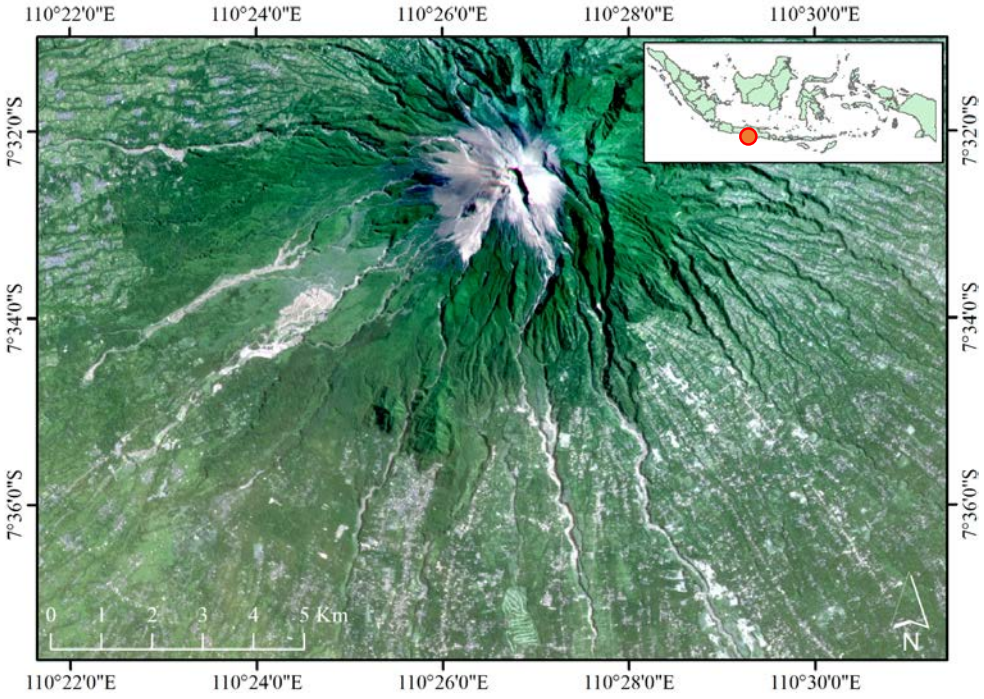

Figure 1. High resolution (3 m) image from the PlanetScope satellite for the area of Mount Merapi and its surroundings displayed with true color composite. Dwellings and agricultural land as close as 5 km from the dome translates in high-level disaster-risk.

 doi:10.20944/preprints202208.0477.v1

The present dome was born from the millennial eruption of 2010 [13], which is topographically resembling a 150 m diameter table-top, which fractured due to phreatic explosions between 2012 and 2014 [4]. Monitoring of volcanoes and dome evolution represents significant technical challenges and risks for the personnel, consequently scientists have been striving to create models and simulations of dome growth and collapses [8], but field-data and evidences are still essential to support those models. Focusing on the period 2012 – 2014, the present contribution proposes to use high-resolution geodetic measurement from airborne LiDAR and from UAV photographs for photogrammetric purposes, in order to detect whether localized deformation and change in the summit area has occurred concomitantly with the dome growth and explosion reported, especially because repeated strain on the crater rim could be the source of volcanic landslide.

2. Materials and Methods

The present contribution includes two sets of data, one LiDAR-based dataset of 2012 and one UAV-dataset of 2014. The 2012 dataset was derived from the airborne LiDAR with a density > 5 point/m^2. The LiteMapper 5600 System was installed on Cessna 402B Aircraft flying at an altitude of 820 m above the summit and the photograph airspeed was 259 km/h. The side-overlap and the frontal-overlap were consecutively 40 % and 60%. GPS surveying for LiDAR base station were concomitantly conducted at Badan Informasi Geospatial (BIG) from reference points using RTK GPS Trimble R9 with minimum 6 satellites. From this dataset, the 2012 data was gridded at a 1 m horizontal resolution, using the minimum vertical value (elevation) in each square-meter grid.

The 2014 dataset was built using Structure from Motion from 328 photographs of 3000x4000 pixels. The photographs were acquired the 16th October 2014 between 12:30 and 12:50 using a fix-wing UAV mounted with a Canon PowerShot S100 of focal length 5 mm and exposure time of 1/1250 seconds and ISO speed of ISO-80. The photographs were integrated into the SfM-MVS (Structure-from-Motion Multiple-View Stereophotogrammetry) software Metashape-Pro commercialized by Agisoft. The process includes the point-cloud reconstruction and its densification. The dense point-cloud was then exported to Cloud Compare, and the point-cloud was subsample at 1 point per square meter to exactly match the point location of the LiDAR data. Using this process, the next step of comparing the two dataset limits the importance of the artefacts linked to variable point density, and also horizontal distance between points. The construction and the modalities of combination of these two datasets are as follows:

The two pointclouds are then aligned in Cloud Compare (Open-source software) to scale the SfM-MVS data and match it to the LiDAR point-cloud using the C2C (Cloud to Cloud) algorithm, from which the distances in the x,y and z directions were separated.

The LiDAR was thus used as the "true elevation", to calibrate the UAV photogrammetry, although error varying based on the type of surface have been reported to vary between 18.9 cm for pavement to 25.9 cm for deciduous tree elevation [23]. Moreover, LiDAR error increases with the slope, and at Mt. Erebus for instance for a slope of 20 degrees' additional vertical error of 16 cm had to be added, reaching locally 21 cm error [24]. In the present case, the authors chose to double those error value and estimate that the LiDAR was accurate to about 50 cm and that any change below this value may not be representative (although all values are reported in the article). The choice to double this value was also motivated by the possibility of sand and ash grains bouncing near the surface, increasing the potential for error.

It resulted in a RMSE (Root Mean Square Error) of 90 cm between the two pointcloud when not taking into account the crater area that is known to have changed. Adding both the error from the aligned 2014 point-cloud to the error assigned to the LiDAR data, the elevation error for the measurements comparing the two surfaces is about 1.4 m.

The dataset from which the authors have worked is thus made of an orthophotographs of the summit in 2014 (Figure 2-a), and two datasets of the dome in 2012 (Figure

Preprints (www.preprints.org) | NOT PEER-REVIEWED | Posted: 29 August 2022 doi:10.20944/preprints202208.0477.v1

2-b) and in 2014 (Figure 2-c). From visual inspection of the hillshaded representation of the DEM one can see the changes that have occurred on the dome (most notably the opening of vents [4]).

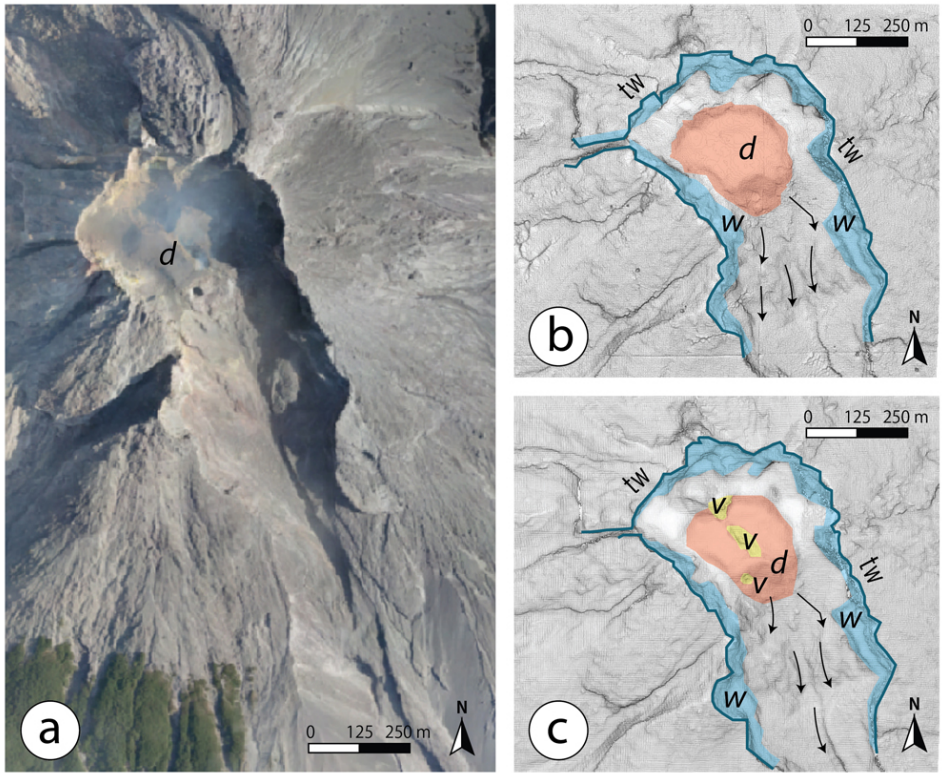

Figure 2. Dome of Merapi Volcano in 2012 and 2014: (a) orthophotograph constructed from UAV imagery in October 2014; (b) Surface map of the dome in 2012 from LiDAR and (c) in 2014 from UAV-SfM-MVS. The captions are (d) dome in transparent red; (v) vent in transparent yellow; (tw) top of the wall and it corresponds to the blue line; (w) wall and it corresponds to the transparent blue

3. Results

The comparison of the two topographic data are presented with first the modifications to the crater rim and the talus and secondly a quantification of the volume removed either from the volcanic explosions or gravitational collapses.

3.1. The crater rim and its talus

At the summit of Mt. Merapi Volcano, a horseshoe crater rim traps the dome. During the period 2012-2014, the crater walls are 100 m to 120 m high above the crater floor at its maximum (North to East-South-East sector), while the West and North sector presents a topographic range of 40 to 80 m (Figure 3). The crater is open to the South. During the period 2012 – 2014, the evolution of the crater rim around the dome is generally stable (no large collapse), although the data shows variation in the geometry of the subvertical walls around the crater rim (b,c,d,e,f,h, and k in figure 3). The walls that spreads outside of the crater rim seem to be more stable (a,l and m in figure 3). At the foot of the crater walls, the topography from 2012 to 2014 is overall stable, showing no major wall collapses, except in e,h and I (figure 3) where the floor level has increased by > 2 m locally. Although the walls seem to show locally large discrepancies between 2012 and 2014 (figure 3-b), the absence of significant deposit at their foot suggest that those are potential artefacts which are examined in the discussion.

Preprints (www.preprints.org) | NOT PEER-REVIEWED | Posted: 29 August 2022 doi:10.20944/preprints202208.0477.v1

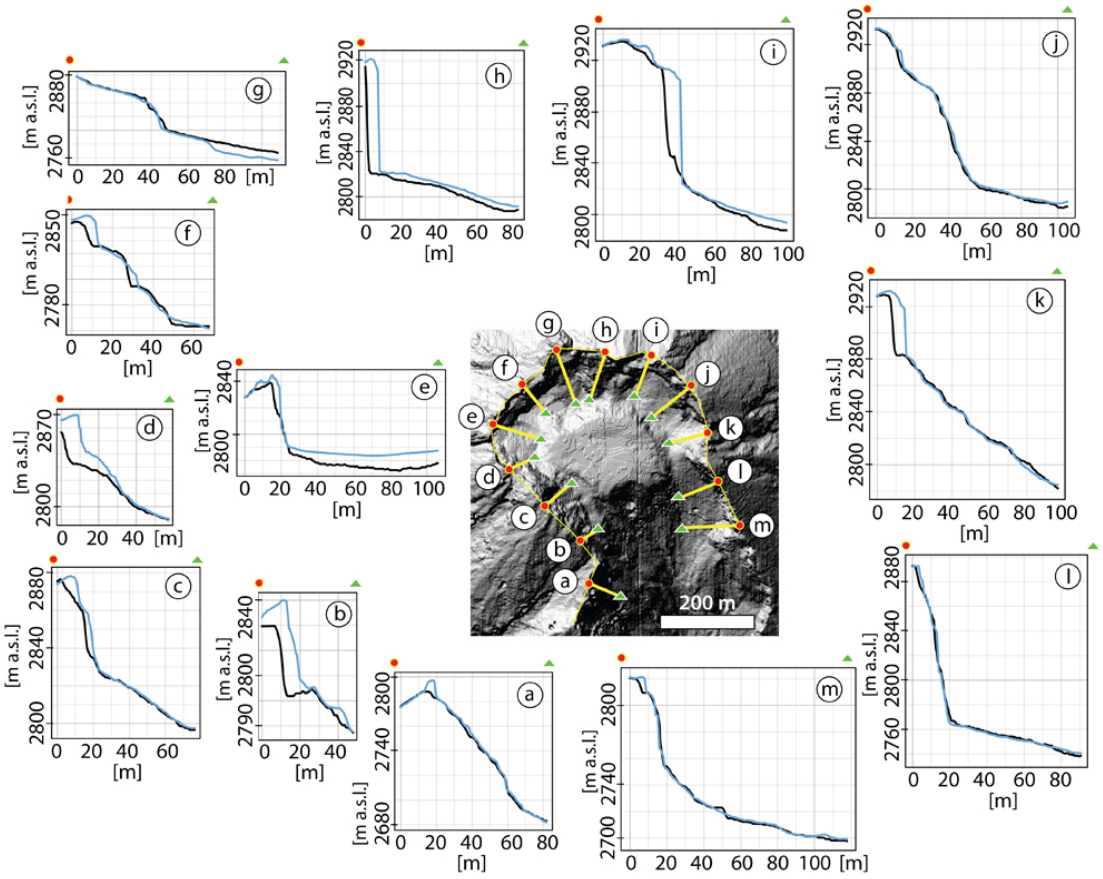

Figure 3. This is a figure. Schemes follow the same formatting (The black line is the topography in 2012 as extracted from the LiDAR-DEM at 1 m horizontal resolution, and the blue line is the topography in 2014, extracted from .the UAV-based photogrammetric model).

3.2. Dome's topographic and volumic change with the localized explosions

As already reported in the literature, during the period 2012 – 2014, the dome locally exploded and split into a set of aligned new vents along a North-West – South-East axis. Around the dome, surface changes also occurred with an increase in elevation (Figure 4). The opening of a new vent on the surface of the dome has displaced an equivalent-volume of 2.04 E+04 m^3 corresponding to a maximum -9 m (+/- 0.9 m) vertically (location 4 on figure 4). At the two vents generated to the North and South of the dome, the volume changes are 2.61 E+05 m^3 (location 2 on figure 4) and 4.82 E+03 m^3 at location 5 (Figure 4). The variability is mostly controlled by the visual depth of the openings (if obstructed by debris, it appears shallows), therefore those values need to be considered as minimal values. Surrounding the plateau created by the dome, loose material is also displaying topographic change. It is mostly increase this time. For the period 2012 to 2014, the rise of material corresponds to respective volume change of 8.56 E+04 m3 at location 1, 1.88 E+04 m3 at location 3 and 6.22 E+04 m3 at location 8. These changes correspond to changes nearing 18 m (+/- 0.9 m) at location 1 and 11 (+/- 0.9 m) m at location 8. On top of these major deformations, gravitational collapses have also been observed on the crater rim (location 10) and a small portion to the South of the dome seem to have also collapsed (location 6 on figure 4).

Preprints (www.preprints.org) | NOT PEER-REVIEWED | Posted: 29 August 2022 doi:10.20944/preprints202208.0477.v1

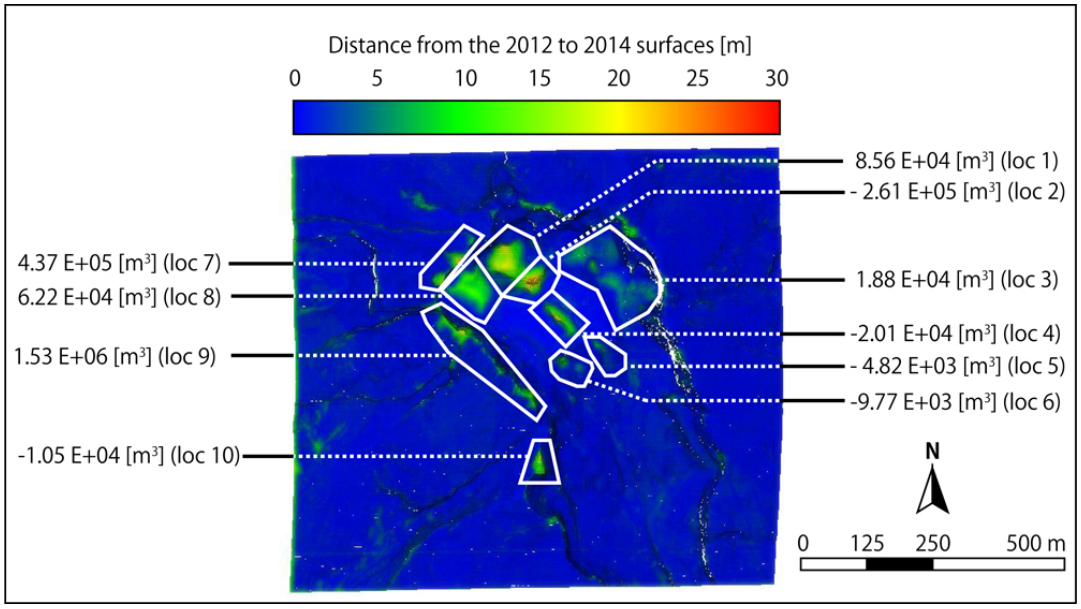

Figure 4. DEM of Difference between the 2012 and 2014 topographic data showing the vents opening and the split in two of the dome, as well as the areas between the crater rim and the dome, where the material was risen. These changes emphasize the changes that are > 2.5 m (i.e. in blue on the map), value above the overall RMSE and the RMSE of the outside structure. This procedure may erase some of the minor variations, but it is aimed at eliminating the false positives from the dataset.

4. Discussion

This discussion is articulated in two sections, with first an interpretation of the results, and what they mean in term of volcanic process, then it follows a section that compares the data of the present contribution with a dataset from 2015, and finally the authors are discussing the implication of the present work for hazards and disaster risk monitoring.

4.1. Surface deformation and interpretation

The dome of Mt. Merapi locally exploded during the period 2012-2014, creating a set of align vents [4], which represents estimated volume of material 2.01 E+04 m^3 for the central elongated vent at the top of the dome, 2.61 E+05 m^3 to the North (high-value determined by a good visibility at a depth of almost 30 m below the pre-explosive surface and one vent to the south, just shy of 1 E+04 m^3. The central elongated vent then represents a topographic drop of about 9 m (Figure 5) although it is most likely that the opening can have been deeper (filled by either ejecta going back to the vent or the full depth being invisible to the SfM-MVS method due to the narrowness of the vent). The origin of these explosions is the result of pressure-increase from the contact with rainwater [4] as well as probable material weakening due to the hydrothermal alteration, a processed that was evidence at the dome summit and its surrounding at a later date [25]. Around the dome, the material, in at least two locations have risen topographically (Figure 5), even without having major wall collapses that would match this rise. If we work by analogy, the dome of 2011, which is visible in 2012 and 2014 may have grown over other extruded material, in the same way the 2017 dome climbed over the 2011 dome [25]. The exploded material may have partly escaped the space of the crater rim, but it is most likely that a large portion of it remained inside the crater, with the largest blocks travelling less distance. Despite a measure of the visible volume change (Figure 4), it is difficult to link both the post-phreatic explosion holes to the deposits, because (1) due to decompression and deposit bulk density changing from the one of the dome, the measured volume change does not reflect a material volume change, (2) part of the material escaped the crater rim, and (3) the post-explosion holes will have certainly collapse and (3) for the deepest part of it ALS

Preprints (www.preprints.org) | NOT PEER-REVIEWED | Posted: 29 August 2022 doi:10.20944/preprints202208.0477.v1

or SfM-MVS may not record the real "bottom" of those. This shows the necessity to develop methodological framework that are more adapted to volcanic vents surveying, due to the numerous complexities it holds. That's why the authors have also added a third existing dataset to try comparing whether "trends" could be seen or whether a visible change may be an artefact.

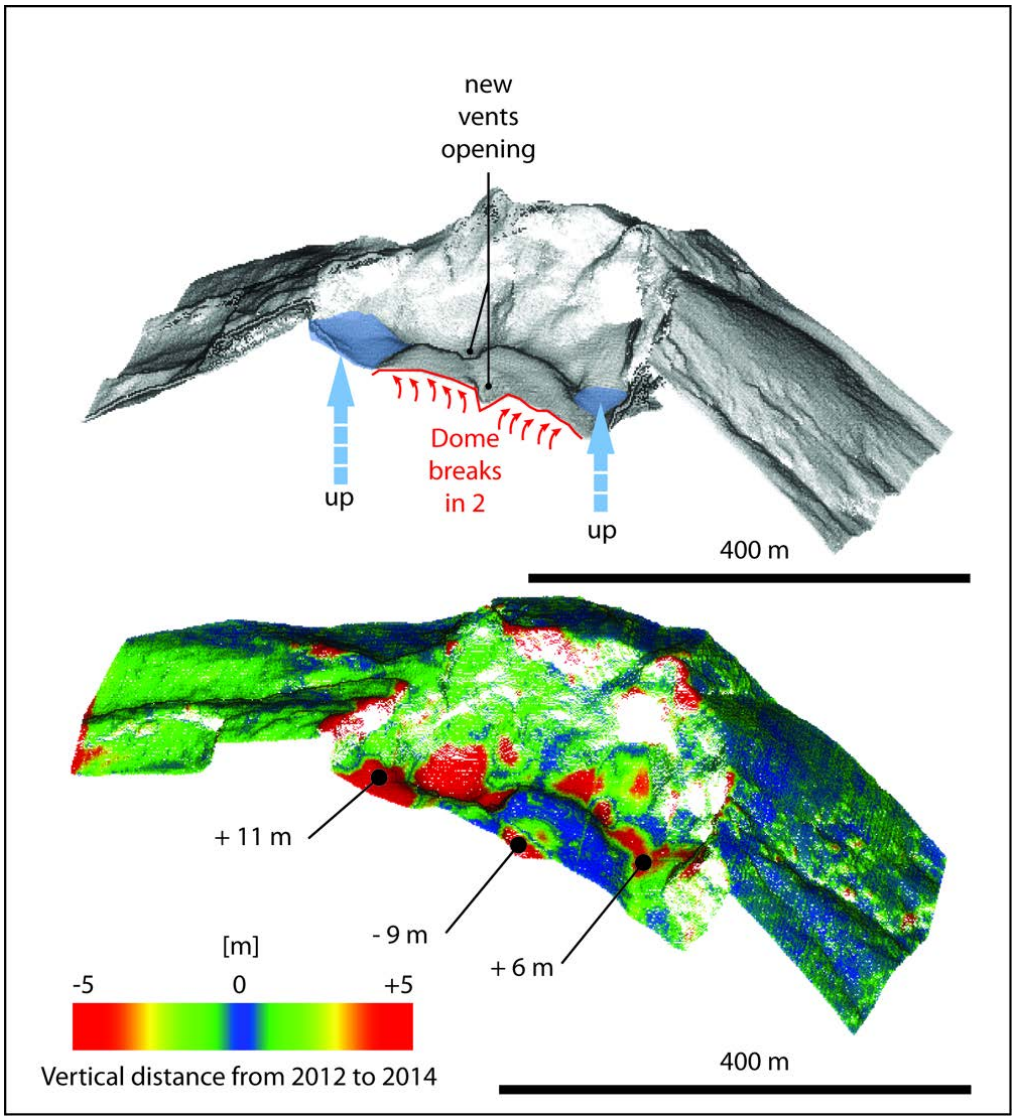

Figure 5. Interpretation figure of the deformation at the dome and near the dome.

4.2. Comparison of the 2012-2014 dataset with the 2015 TLS and SfM-MVS acquired data

Combining laser-scanner and photogrammetric methods, a 3D pointcloud of the dome was generated in 2015 was compared to the 2012 and 2014 dataset presented in this study (Figure 6). Looking at the dome in the center, the topography of 2012 and 2014 is overall slightly higher than the value of 2015, which could be either a general shrinking as it happens between different eruptive phases or a generalized error, the two being difficult to separate from one another, because of the difficult conditions of data acquisition. A similar pattern can also be seen on the outer area of the crater rim, but as it represents the periphery of the 2015 dataset and as the 2012 and 2014 are well-aligned, it is likely that

Preprints (www.preprints.org) | NOT PEER-REVIEWED | Posted: 29 August 2022 doi:10.20944/preprints202208.0477.v1

error emerged in the outer part of the crater rim on the 2015 dataset. Mindful of the potential error, there are however topographic trends that emerge. For instance, at 80 degrees' direction (Figure 6), the topographic wall is moving inward with large blocks with a crack in its center appearing. This large portion of the subvertical wall is likely to collapse onto the crater floor and the dome. In areas that are difficult to access, repeating the same measure several times (for instance using a drone) is certainly one way to reduce the uncertainty due to the data acquisition and processing process (which in photogrammetry is directly linked to the photographs and their characteristics).

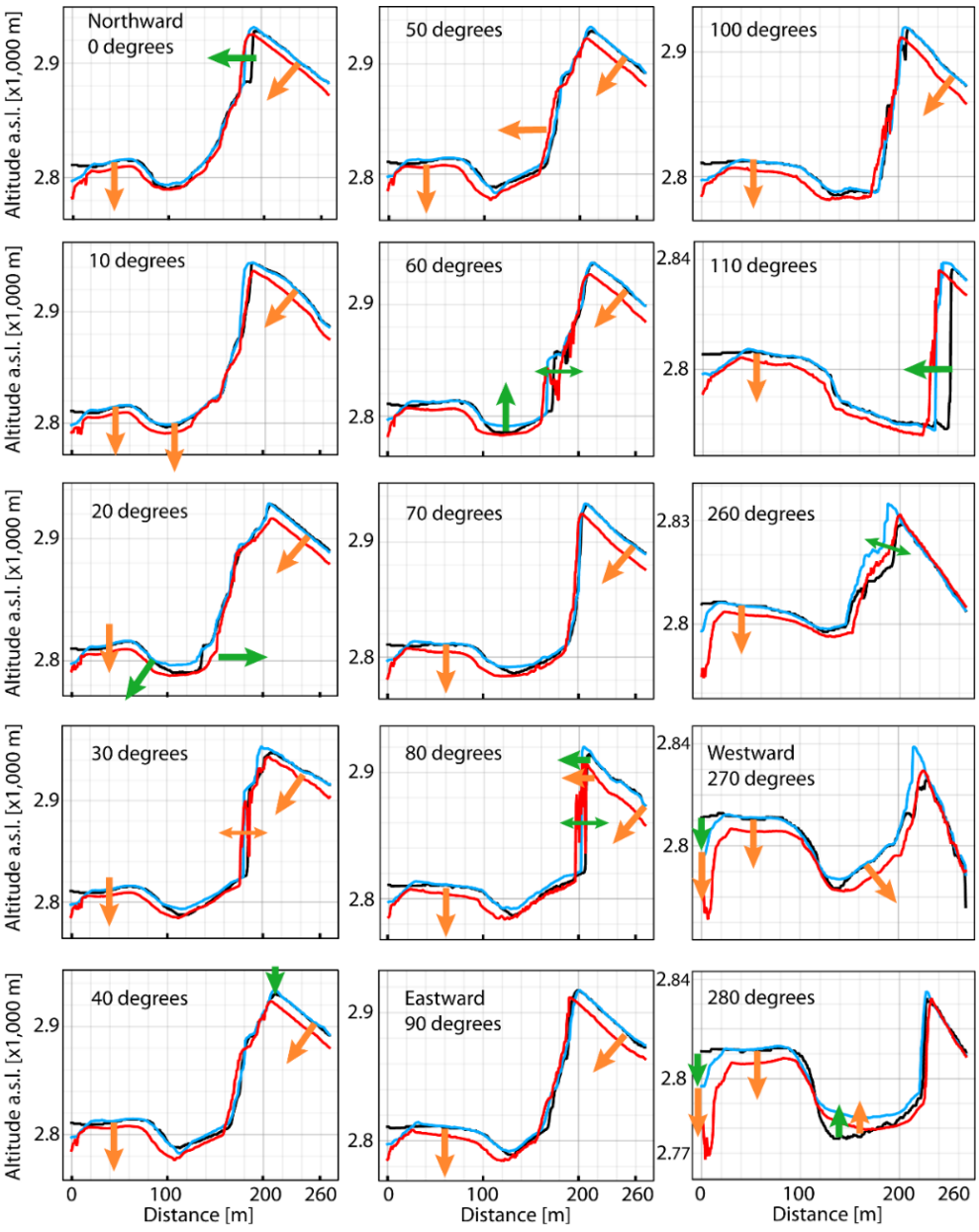

Figure 6. Comparison of the data from the present research with the data of Damarawan et al., 2018, provided as supplementary data [26]. The degrees represent transect orientation rotating from the center of the dome in a clockwise direction, starting at 0 degrees being the North. The main cardinal orientations are also provided (the southern opening is not represented). The black lines represent the 2012 topography, the blue line, the 2014 topography and the red line is the 2015 topography. The orange arrows show a significant difference in topography between 2014 and 2015, and the green arrows between 2012 and 2015 (so that 2014 is in a transition phase between the two surfaces or moved during the 2012-2014 period).

5. Conclusion

The main conclusions of the present paper are that (1) during the period 2012 – 2014 when the dome of Merapi experienced phreatic or phreatomagmatic explosions, the topography around the dome rose; (2) this rise does not seem to be related to large wall collapses, and it is likely that modification in the subsurface have triggered those changes; (3) from a technical perspective, there is a need to develop UAV imagery acquisition methods that are fit for volcanic craters, with step walls (e.g. avoiding NADIR images), in order to reduce the error due to the lack of data notably.

Supplementary Materials: The following supporting information can be downloaded at: www.mdpi.com/xxx/s1, Figure S1: title; Table S1: title; Video S1: title.

Author Contributions: The first author drafted the paper and all the authors have contributed to the final write-up. The data were collected by the members of UGM in Indonesia. The members from UGM worked to construct the SfM and the LiDAR data, as well as the ground survey to obtain the survey points. The team from Japan worked on the processing and the alignment of the dataset. The data and construction of information was discussed among the members. FL further provided extensive writing advices and background information.

Funding: This research was funded by Riset Kolaborasi Indonesia (RKI) number 1545/UN1/DITLIT/Dit-Lit/PT.01.03/2022. The authors also thank two anonymous reviewers and the editor for their valuable comments to strengthen this paper. Further funding was provided at Kobe University through the IMARC international program on volcanic hazards lead by Prof. C. Gomez.

Data Availability Statement: All the data used in the present contribution can be accessed upon contacting the corresponding author.

Acknowledgments: N.A.

Conflicts of Interest: The authors declare no conflict of interest.

References

1. Voight, B.; Elsworth, D. Instability and collapse of hazardous gas-pressurized lava-domes. *Geophys Res Let* **2000** *27*, 1-4.
2. Swanson, D.A.; Holcomb, R.T. Regularities in Growth of the Mount St. Helens Dacite Dome, 1980-1986. *IAVCEI Proceedings – Lava Flows and Domes* **1990** *2* 3-24.
3. Loughlin, S.C.; Calder, E.S.; Clarke, A.; Cole, P.D.; Luckett, R.; Mangan, M.T.; Pyle, D.M.; Sparks, R.S.J.; Voight, B.; Watts, R.B. Pyroclastic flows and surges generated by the 25 June 1997 dome collapse, Soufriere Hills Volcano, Montserrat. In *The Eruption of Soufriere Hills Volcano, Montserrat, from 1995 to 1999*, Druit, T.H., Kokelaar, B.P. Eds.; Publisher: Geological Society, London, United-Kingdom; 1990. Volume 21, pp. 129-209.
4. Darmawan, H.; Walter, T.R.; Troll, V.R.; Budi-Santoso, A. Structural weakening of the Merapi dome identified by drone photogrammetry after the 2010 eruption. *Nat. Hazards Earth Syst. Sci.* **2018** *18*
5. Gomez, C.; Allouis, C.; Lissak, N.; Hotta, N.; Shinohara, Y.; Hadmokok, D.S.; Vilimek, V.; Wassmer, P.; Lavigne, F.; Setiawan, A.; Sartohadi, J.; Saputra, A.; Rahardianto, T. High-Reolustion Point-Cloud for Landslides in the 21st Century: From Data Acquisition to New Processing Concepts, In *Understanding and Reducing Landslide Disaster* Risk; Arbanas Z. et al. Eds.; 2021. Springer Nature, Switzeraland; 2021. Volume 6, pp. 199-213.
6. Darmawan, H.; Yuliantoro, P.; Rakhman, A., Santoso, A.B.; Humaida, H.; Suryanto, W. Dynamic velocity and seismic characteristics of gravitational rockfalls at the Merapi lava dome. *J Volcanol Geotherm Res* **2020** *404*, 107010, 1-10.
7. Vazquez, R.; Macias, J.L.; Alcala-Reygosa, J.; Arce, J.L.; Jimenez-Haro, A.; Fernandez, S.; Carlon, T.; Saucedo, R.; Sanchez-Nunez, J.M. Numerical modeling and hazard implications of landslides at the Ardillas Volcanic Dome (Tacana Volcanic Complex, Mexico-Guatemala). *Nat Hazards* **2022** doi.org/10.1007/s11069-022-05348-1, pp 1-28.
8. Kelfoun, K.; Santoso, A.B.; Latchimy; T.; Bontemps, M.; Nurdienm I.; Beauducel, F.; Fahmi, A.; Putra, R.; Dahamna, N.; Laurin, A.; Rizal, M.H.; Suksmana, J.T.; Gueugneau, V. Growth and collapse of the 2018-2019 lava dome of Merapi Volcano. *Bull Volcanol* **2021** *83*, pp 1-13.
9. Gomez, C.; Janin, M.; Lavigne, F.; Gertisser, R.; Charbonnier, S.; Lahitte, P.; Hadmoko, D.S.; Fort, M.; Wassmer, P.; Degroot, V.; Murwanto, H. Borobudur, a basin under volcanic influence: 361,000 years BP to present. *J Volcanol Geotherm Res* **2010** *196*, 2545-264.
10. Newhall, C.G.; Bronto, S.; Alloway, B.; Banks, N.G.; Bahar, I.; del Marmol, M.A.; Hadisantono, R.D.; Holcomb, R.T.; McGeehin, J.; Miksic, J.N.; Rubin, J.N.; Sayudin, S.D.; Sukhyar, R.; Andreastuti, S.; Tilling, R.I.; Torley, R.; Trimble, D.; Wirakusumah, A.D. 10,000 years of explosive eruptions of Merapi Volcano, Central Java: archeological and modern implications. *J Volcnaol Geothermal Res* **2000** *100*, 9-50.

11. Surono; Jousset P.; Pallister J.; Boichu M.; Buongiorno M.; Budisantoso A.; Costa F.; Andreastuti S.; Prata F.; Schneider D.; Lieven C.; Humaida H.; Sri Sumarti; Bignami C.; Griswold J.; Carn S.; Oppenheimer C.; Lavigne F. The 2010 explosive eruption of Java's Merapi volcano – a '100-year' event. *J Volcnaol Geothermal Res* **2012**, *241–242*, 121-135.
12. Charbonnier, S.J.; Germa, A.; Connor, C.B.; Gertisser, R.; Preece, K.; Komorowski, J.-C.; Lavigne, F.; Dixon, T.; Connor, L. Evaluation of the impact of the 2010 pyroclastic density currents at Merapi volcano from high-resolution satellite imagery, field investigations and numerical simulations. *J Volcanol Geotherm Res* **2013** *261*, 295-315.
13. De Belizal E.; Lavigne F.; Robin A.K.; Sri Hadmoko D.; Cholik N.; Thouret J.C.; Sawudi D.S.; Muzani M.; Sartohadi J.; Vidal C.; 2013. Rain-triggered lahars following the 2010 eruption of Merapi volcano, Indonesia: A major risk. *Volcanol Geotherm Res* **2013** *261*, 330-347.
14. Komorowski, J.-C.; Jenkins, S.; Baxter, P.J.; Picquout, A.; Lavigne, F.; Charbonnier, S.; Gertisser, R.; Preece, K.; Cholik, N.; Budi-Santo, A.; Surono. Paroxysmal dome explosion during the Merapi 2010 eruption: processes and facies relationships of associated high-energy pyroclastic density currents. *J Volcanol Geotherm Res* **2013** *261*, 260-294.
15. Sri Hadmoko, D.; de Belizal, E.; Mutaqin, B.W.; Dipayana, G.A.; Marfai, M.A.; Lavigne, F.; Sartohdai, J.; Worosuprojo, S.; Starheim, C.A.; Gomez, C. Post-eruptive lahars at Kali Putih following the 2010 eruption of Merapi Volcano, Indonesia: occurrences and impacts. *Nat Hazards* **2018** *94*, 419-444.
16. Allard, P. Proportions des isotopes 13 C et 12 C du carbone émis à haute température par un dome andésitique en cours de croissance; Le Merapi (Indonésie) -- Proportions of C-13 and C-12 isotopes of carbon emitted at high temperature by an andesitic dome during growth; Merapi, Indonesia, *C. R. Acad. Sci., Série D* **1980**, *291:7*, 613-616.
17. Le Guern, F.; Gerlach, T. M.; Nohl, A., Field gas chromatograph analyses of gases from a glowing dome at Merapi Volcano, Java, Indonesia, 1977, 1978, 1979, *J. Volcanol. Geotherm. Res.* **1982** *14:3-4*, 223-245.
18. Kelfoun, K., Processus de croissance et de déstabilisation des dômes de lave du volcan Merapi (Java Centrale, Indonésie). Modélisations numériques des dômes, dynamique des écoulements pyroclastiques associés et surveillance par stéréophotogrammétrie, PhD thesis, Univ. Blaise Pascal Clermont-Ferrand II, **1999**.
19. Clocchiatti, R.; Joron, J.-L.; Kerinec, F.; Treuil, M., Quelques données préliminaires sur la lave du dome actuel du volcan Merapi (Java, Indonésie) et sur ses enclaves - Preliminary data on lava from the present dome of the volcano Merapi (Java, Indonesia) and on its xenoliths, *C. R. Acad. Sci., Série 2*, **1982**, *295:9*, 817-822.
20. Voight, B., Young, K.D., Hidayat, D. Deformation and seismic precursors to dome-collapse and fountain-collapse nuées ardentes at Merapi Volcano, Java, Indonesia, 1994--1998, *J. Volcanol. Geotherm. Res.*, special issue Merapi volcano **2000** *100:1-4*, 261-287.
21. Young, K.D., Voight, B. Ground deformation at Merapi Volcano, Java, Indonesia: distance changes, June 1988--October 1995, J. *Volcanol. Geotherm. Res.*, special issue Merapi volcano **2000** *100:1-4*, 233-259.
22. Brodscholl, A.; Kirbani, S.B.; Voight, B,. Sequential dome-collapse nuées ardentes analyzed from broadband seismic data, Merapi Volcano, Indonesia, *J. Volcanol. Geotherm. Res.*, special issue Merapi volcano **2000** *100:1-4*, 363-369.
23. Hodgson, M.E.; Bresnahan, P. Accuracy of Airborne Lidar-Derived Elevation: Empirical Assessment and Error Budget. *Photogram Eng Remote Sens* **2004** *70*, 331-339.
24. Csatho, B.; Schenck, T.; Kyle, P.; Wilson, T.; Krabill, W.B. Airborne laser swath mapping of the summit of Erebus volcano, Antarctica: Applications to geological mapping of a volcano. *J Volcanol Geotherm Res* **2008** *177*, 531-548.
25. Darmawan, H.; Troll, V.R.; Walter, T.R.; Deegan, F.M.; Geiger, H.; Heap, M.J.; Seraphine, N.; Harris, C.; Humaida, H.; Muller, D. Hidden mechanical weaknesses within lava domes provided by buried high-porosity hydrothermal alteration zones. *Scientific Reports* **2022** *13-302*, 1-14.
26. Darmawan, H.; Walter, T.; Richter, N.; Nikkoo, M. High resolution Digital Elevation Model of Merapi summit in 2015 generated by UAVs and TLS. V. 2015. **2017** *GFZ Data Services*. https://doi.org/10.5880/GFZ.2.1.2017.003